



## M2 exosomes modified by hydrogen sulfide promoted bone regeneration by moesin mediated endocytosis

Yi-kun Zhou<sup>a,b,c,1</sup>, Chun-shan Han<sup>a,b,c,1</sup>, Zi-lu Zhu<sup>a,b,c,1</sup>, Peng Chen<sup>a,b,c</sup>, Yi-ming Wang<sup>a,b,c</sup>,  
Shuai Lin<sup>a,b,c</sup>, Liu-jing Chen<sup>a,b,c</sup>, Zi-meng Zhuang<sup>a,b,c</sup>, Yan-heng Zhou<sup>a,b,c</sup>, Rui-li Yang<sup>a,b,c,\*</sup>

<sup>a</sup> Department of Orthodontics, Peking University School and Hospital of Stomatology, Haidian District, Beijing, China

<sup>b</sup> National Clinical Research Center for Oral Diseases & National Engineering Laboratory for Digital and Material Technology of Stomatology, Haidian District, Beijing, China

<sup>c</sup> Beijing Key Laboratory of Digital Stomatology, Haidian District, Beijing, China

### ARTICLE INFO

#### Keywords:

Macrophages

Exosomes

Bone regeneration

Stem cells

Hydrogen sulfide

Moesin

### ABSTRACT

Bone defects caused by trauma or tumor led to high medical costs and poor life quality for patients. The exosomes, micro vesicles of 30–150 nm in diameter, derived from macrophages manipulated bone regeneration. However, the role of hydrogen sulfide (H<sub>2</sub>S) in the biogenesis and function of exosomes and its effects on bone regeneration remains elusive. In this study, we used H<sub>2</sub>S slow releasing donor GYY4137 to stimulate macrophages and found that H<sub>2</sub>S promoted the polarization of M2 macrophages to increase bone regeneration of MSCs *in vitro* and *in vivo*. Moreover, we developed the H<sub>2</sub>S pre-treated M2 macrophage exosomes and found these exosomes displayed significantly higher capacity to promote bone regeneration in calvarial bone defects by re-establishing the local immune microenvironment. Mechanically, H<sub>2</sub>S treatment altered the protein profile of exosomes derived from M2 macrophages. One of the significantly enriched exosomal proteins stimulated by H<sub>2</sub>S, moesin protein, facilitated the exosomes endocytosis into MSCs, leading to activated the  $\beta$ -catenin signaling pathway to promote osteogenic differentiation of MSCs. In summary, H<sub>2</sub>S pretreated M2 exosomes promoted the bone regeneration of MSCs *via* facilitating exosomes uptake by MSCs and activate  $\beta$ -catenin signaling pathway. This study not only provides new strategies for promoting bone regeneration, but also provides new insights for the effect and mechanism of exosomes internalization.

### 1. Introduction

Large scale bone defects severely compromised the esthetics and musculoskeletal functions of patients, which led to high medical costs to individuals and society. Mesenchymal stem cells (MSCs) based regenerative medicine is a promising approach for bone regeneration. While the immune response and inflammation in the local environment play a key role in the bone regeneration or healing of bone fracture [1]. It's reported that proinflammatory cytokines regulated the characteristics of stem cells to repair bone injuries [2,3]. In early bone fracture healing, acute inflammation leads to the production of chemokines such as CXCL12–CXCR4 crosstalk and IL-6 to stimulate osteoblastic differentiation of MSCs, which accelerates bone formation [4,5]. However, the

cytokines tumor necrosis factor- $\alpha$  (TNF- $\alpha$ ) and interferon- $\gamma$  (IFN- $\gamma$ ) combination treatment induced MSC apoptosis and inhibited MSC-based bone regeneration [6]. In periodontitis, chronic inflammation can inhibit osteoblastic cells to form new bones mediated by TNF- $\alpha$ , and another pro-inflammatory milieu [7]. Thus, it's important to establish the proper local immune microenvironment to achieve bona fide bone regeneration.

Macrophages play important roles in mediating inflammation because of their remarkable plasticity to polarize into two distinct subtypes M1 and M2 macrophages on different stimulus [8,9]. M2 macrophages are crucial for anti-inflammatory to enhance bone regeneration of MSCs [8]. However, the direct use of M2 macrophages has notable disadvantages, such as time-consuming cell culture process, phenotype

Peer review under responsibility of KeAi Communications Co., Ltd.

\* Corresponding author. Department of Orthodontics, Peking University School and Hospital of Stomatology, 22 Zhongguancun Avenue South, Haidian District, Beijing, 100081, China.

E-mail addresses: [ruiyang@bjmu.edu.cn](mailto:ruiyang@bjmu.edu.cn), [ruiyangabc@163.com](mailto:ruiyangabc@163.com) (R.-l. Yang).

<sup>1</sup> These authors contributed equally.

<https://doi.org/10.1016/j.bioactmat.2023.08.006>

Received 29 March 2023; Received in revised form 31 July 2023; Accepted 8 August 2023

2452-199X/© 2023 The Authors. Publishing services by Elsevier B.V. on behalf of KeAi Communications Co. Ltd. This is an open access article under the CC BY-NC-ND license (<http://creativecommons.org/licenses/by-nc-nd/4.0/>).

changes during cell expansion, and low survival rate of locally transplanted cells. Recent evidence indicated that the effects of macrophages control bone physiology was largely facilitated *via* the paracrine mechanism [10]. Cellular interactions also involve the components of secretomes. Exosomes, with an average diameter of 30–150 nm, secreted by a variety of cells and endocytosed by target cells to regulate their biology. Macrophage exosomes play a role in varied physiological and pathological conditions, such as immune response, infection, cancer and tissue injury [11]. It's reported that macrophage exosome treatment enhanced the osteoinduction of cultured MSCs [12], however, the exact effects and the cellular interaction mechanism remains unclear.

Hydrogen sulfide (H<sub>2</sub>S), the third gaseous signaling molecule except nitric oxide, and carbon monoxide [1], plays an important role in inflammation and immune response. It has been reported to exert both pro-inflammatory and anti-inflammatory effects [13]. H<sub>2</sub>S is important for T cell activation, Treg cell differentiation and stability *via* protein sulphydration [14]. Recent studies also showed that H<sub>2</sub>S signaling plays a key role in indicating macrophage polarizations. The endogenous H<sub>2</sub>S was reported to attenuate LPS-induced oxidative stress and inflammatory damage by suppressing the NOX4-ROS pathway in macrophages [15,16]. GYY4137, an H<sub>2</sub>S-slow-releasing molecule, was reported to suppress macrophage M1 polarization to inhibit rat endotoxic shock and mucosal wound [17]. H<sub>2</sub>S could promote macrophage migration and M2 macrophage polarization by enhancing mitochondrial biogenesis and fatty acid oxidation (FAO), which may accelerate post myocardial infarction recovery [18]. It was reported that bone marrow MSCs can generate H<sub>2</sub>S endogenously to regulate their self-renewal and osteogenic differentiation through calcium channels [19]. However, whether H<sub>2</sub>S could regulate the local immune response and inflammation to provide a proper microenvironment to facilitate osteogenic differentiation remains unclear.

Here, our study demonstrated that H<sub>2</sub>S promoted the polarization of M2 macrophages and alter exosomal protein profile, with highly enriched of the exosomal moesin protein, which facilitates the exosomes endocytosis into MSCs. The H<sub>2</sub>S pretreated M2 exosomes promoted bone regeneration by re-establishing the local immune microenvironment.

## 2. Results

### 2.1. H<sub>2</sub>S facilitated macrophage polarization into M2 subtype

Firstly, we tested the role of H<sub>2</sub>S on the M2 polarization of macrophages. We found that H<sub>2</sub>S donor GYY4137 treatment promoted M2 macrophage polarization in the IL-4 induction condition by increased the ratio of CD115<sup>+</sup>F4/80<sup>+</sup> cells, as assessed by flow cytometry (Fig. 1A). Moreover, H<sub>2</sub>S donor treatment increased the expression of arginase-1(Arg-1), as assessed by qPCR, western blot and immunofluorescence staining (Fig. 1B–D). However, H<sub>2</sub>S treatment failed to alter the polarization of M1 macrophages (Fig. 1E). As the expression of iNOS was elevated by LPS treatment, but not altered by H<sub>2</sub>S treatment assessed by qPCR, western blot and immunofluorescence, respectively (Fig. 1F–H). We also found that H<sub>2</sub>S could promote the proportion of morphological changes in macrophages compared with IL-4 induction (Supplementary Fig. 1A and 1B), but not altered with LPS induction (Supplementary Fig. 1C). These results showed that H<sub>2</sub>S promoted the polarization of macrophages to the M2 subtype, but had no significant effect on M1 macrophage polarization.

### 2.2. H<sub>2</sub>S stimulated-macrophage conditioned medium promoted osteogenic differentiation of MSCs

It was reported that M2 macrophages could promoted the osteogenic differentiation of MSCs *via* paracrine secreted cytokines [20]. To analyze whether H<sub>2</sub>S treatment regulates the effects of M2 macrophages on bone regeneration, we used M2 macrophage-conditioned medium and GYY4137 pretreated M2 macrophage conditioned medium to treat

MSCs. The results showed that osteogenic differentiation of MSCs was increased after H<sub>2</sub>S pretreated-M2 medium treatment, as showed by alkaline phosphatase (ALP) and alizarin red S staining (Fig. 2A and B). Moreover, the expression of ALP and Runx2 was significantly increased after treated with H<sub>2</sub>S pretreated-M2 medium, compared with M2 medium (Fig. 2C and D). These results showed that H<sub>2</sub>S regulated the macrophage paracrine pathways to promote osteogenic differentiation of MSCs.

### 2.3. H<sub>2</sub>S treatment promoted exosome endocytosis by MSCs

To invest the impacts of H<sub>2</sub>S on the exosomes of macrophages, we separated the exosomes from macrophages (M0-exo), M2 macrophages (M2-exo) and H<sub>2</sub>S pretreated-M2 macrophages (GYY-M2-exo) and analyzed the expression of CD63 and CD81 in these exosomes. The results showed that no significant difference was detected among the three groups (Fig. 3A). Then, the number and diameters of different exosomes were compared by nanoparticle tracing analysis (NTA) and transmission electron microscope (TEM). The results showed that there is no difference about the quantity and diameter of exosomes derived from these different treated macrophages (Fig. 3B–D). Then the mass spectrometry was used to analyze the protein profile of exosomes from different treatment macrophages to clarify how H<sub>2</sub>S regulates the capacity of exosomes. The heatmap depicted the significant (fold change >2, *p* < 0.05) upregulated and downregulated proteins (Fig. 3E, and Supplementary Fig. 2A). Then the function of the different proteins was analyzed by using Gene Ontology (GO) and Biological Process (BP) enrichment while the results showed that the positive regulation of protein transport and positive regulation of endocytosis were among the top ten enriched clusters (Fig. 3F and G). To analyze the role of H<sub>2</sub>S in exosome endocytosis, we labeled exosomes with PKH26 to treat MSCs. The results showed that the endocytic exosomes, shown by red fluorescence, significantly increased in the H<sub>2</sub>S pre-treatment group, indicating that H<sub>2</sub>S promoted the exosome uptake by MSCs. The internalized exosomes were visualized as dots of red fluorescence around the MSCs nuclei in a time-dependent manner (Fig. 3H and I, Supplementary Fig. 2B and Supplementary video). We further quantitatively measured the cellular uptake of exosomes at 12h using flow cytometry and the results showed that more M2 exosomes were uptaken by MSCs than M0 exosomes. Moreover, H<sub>2</sub>S pretreatment could enhance the exosomes endocytosis by MSCs than M2 exosomes (Fig. 3J). These results indicated that H<sub>2</sub>S treatment increased endocytosis of exosomes.

### 2.4. H<sub>2</sub>S pretreated exosomes promoted osteogenic differentiation of MSCs

To verify the effects of H<sub>2</sub>S pretreated exosomes on osteogenic differentiation of MSCs, the exosomes from M2 macrophages and H<sub>2</sub>S pretreated-M2 macrophages were collected to treat MSCs. The results showed that M2 exosomes treatment could promote osteogenic differentiation of MSCs compared to the control group. Moreover, H<sub>2</sub>S pretreated-M2 exosomes treatment group showed significantly superior osteogenic differentiation capacity compared with M2 exosomes treatment group, as assessed by ALP staining and Alizarin red staining (Fig. 4A and B). The expression of ALP and Runx2 in MSCs were significantly elevated after H<sub>2</sub>S pretreated M2 exosomes treatment compared with M2 exosomes treatment group. (Fig. 4C–E). To verify the role of H<sub>2</sub>S on bone regeneration *in vivo*, 4 × 10<sup>6</sup> MSCs were mixed with hydroxyapatite/tricalcium phosphate (HA/TCP) as a scaffold and subcutaneously implanted into the dorsal of immunocompromised mice. The results showed more new bone formation in the M2 exosomes treatment group compared with the control group. Furthermore, H<sub>2</sub>S pretreatment significantly enhanced new bone formation compared with the M2 exosomes treatment with more Arg-1 positive M2 macrophages in bone tissue formation area in the H<sub>2</sub>S pretreated-M2 exosomes treatment group (Fig. 4F). There were more ALP and Runx2 positive

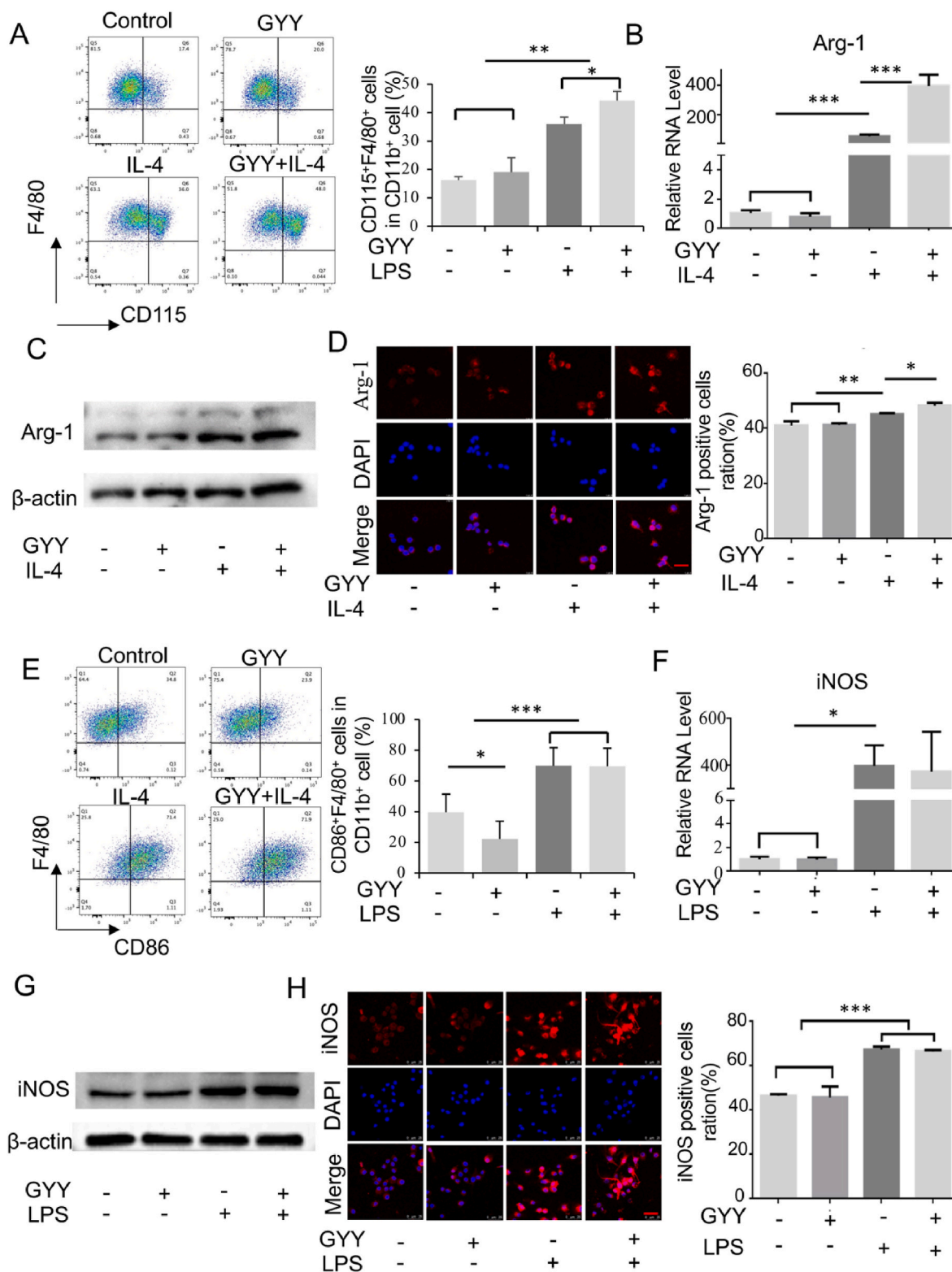


**Fig. 1.** H<sub>2</sub>S facilitated macrophage polarization toward the M2 subtype. (A) The ratio of CD115<sup>+</sup>F4/80<sup>+</sup> cells in control, IL-4 (50 ng/ml), GYY4137 (50 μM), and IL-4 and GYY4137 combination treated 24h groups, as assessed by flow cytometry. (B, C) The expression of Arg-1 in control, IL-4, GYY4137, and IL-4 and GYY4137 combination treatment groups, as assessed by qPCR (B) and western blot (C). (D) The expression of Arg-1 in control, IL-4, GYY4137, and IL-4 and GYY4137 combination treatment macrophages, as assessed by immunofluorescent staining. (E) The ratio of CD86<sup>+</sup>F4/80<sup>+</sup> cells in control, LPS (50 ng/ml), GYY4137, and LPS and GYY4137 combination treatment groups, as assessed by flow cytometry. (F–H) The expression of iNOS in control, LPS, GYY4137, and LPS and GYY4137 combination treated macrophages, as assessed by qPCR (F), western blot (G) and Immunofluorescent staining (H). Scale bars, 25 μm. GYY: GYY4137, data are presented by mean ± SD (\*P < 0.05, \*\*P < 0.01, \*\*\*p < 0.001).

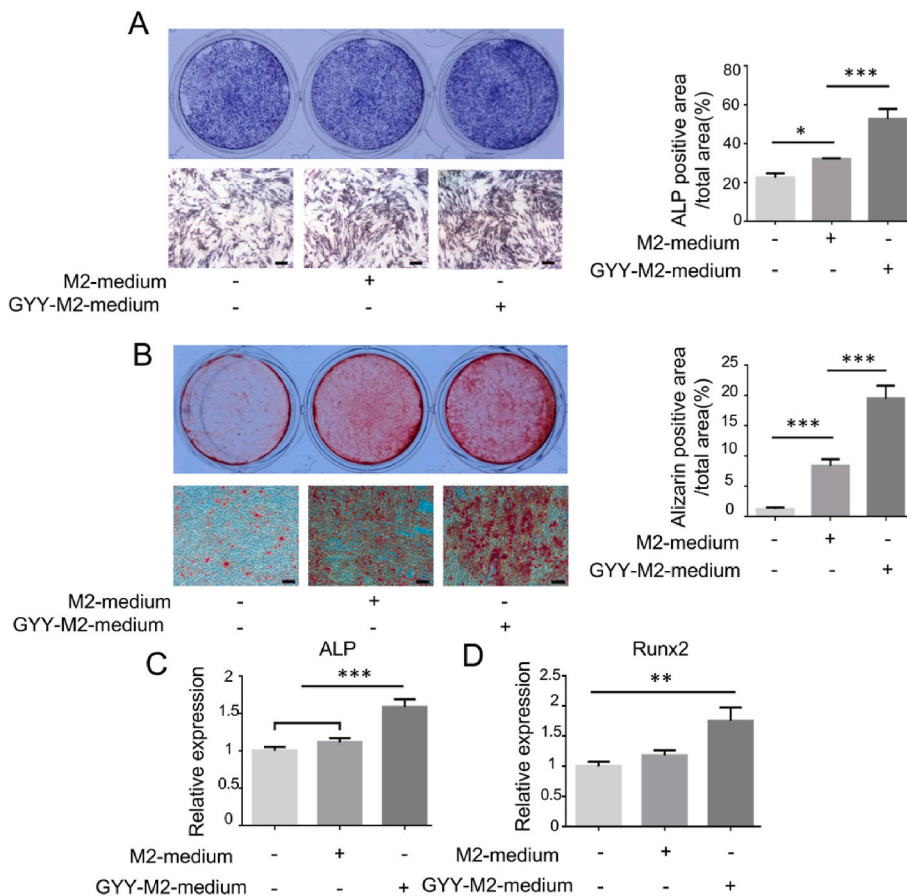


**Fig. 2.** H<sub>2</sub>S pretreated-macrophage conditioned medium promoted osteogenic differentiation of MSCs. (A) Alkaline phosphatase staining showed the ALP positive osteoblastic colonies in control, M2 macrophage conditioned medium, and H<sub>2</sub>S pretreated-M2 macrophage conditioned medium treatment groups. (B) The mineralized nodule formation of MSCs treated by M2 macrophage conditioned medium and H<sub>2</sub>S pretreated-M2 macrophage conditioned medium, as assessed by Alizarin red staining. (C-D) The expression of ALP and Runx2 of MSCs in control, M2 macrophage conditioned medium, and H<sub>2</sub>S pretreated-M2 macrophage conditioned medium treatment groups, as assessed by qPCR analysis. Scale bars, 10  $\mu$ m. Data are presented by mean  $\pm$  SD (\*P < 0.05, \*\*P < 0.01, \*\*\*P < 0.001).

cells detected in the new bone formation area in H<sub>2</sub>S pretreated-M2 exosomes treatment group, as assessed by immunofluorescence staining (Fig. 4G and H). These results indicated that H<sub>2</sub>S pretreated M2 exosomes promoted osteogenic differentiation of MSCs *in vitro* and *in vivo*.

### 2.5. H<sub>2</sub>S pretreated exosomes enhanced calvarial bone defects regeneration

To verify the effects of H<sub>2</sub>S pretreated exosomes on bone regeneration, we used M2 exosomes and H<sub>2</sub>S pretreated M2 exosomes to treat critical size calvarial bone defects and the results showed that M2 exosomes could promote calvarial bone regeneration. While the calvarial bone defects regeneration is significantly superior in H<sub>2</sub>S pretreated M2 exosomes group than the M2 exosomes group, as assessed by Micro-CT (Fig. 5A and B and Supplementary Fig. 3A and 3B). Moreover, the calvarial bone structure in H<sub>2</sub>S pretreated M2 exosomes group is more regular as like the natural bone, compared with the M2 exosomes group, as assessed by HE staining (Fig. 5C). The expression of ALP and Runx2 were also significantly higher in H<sub>2</sub>S pretreated M2 exosomes group than M2 exosomes group (Fig. 5D and E). Furthermore, there were more Arg-1 positive macrophages enriched in the bone regeneration area of H<sub>2</sub>S pretreated M2 exosomes group than the M2 exosomes group (Fig. 5F). These results verified the effects of H<sub>2</sub>S pretreated exosomes to promote bone regeneration. In order to verify the effects of H<sub>2</sub>S on bone regeneration, we created the calvaria bone defects in control and *Cbs*<sup>-/-</sup> mice to compare their regeneration capacity. The results showed that the regeneration capacity of *Cbs*<sup>-/-</sup> mice is inferior than the WT mice as assessed by Micro-CT and HE staining (Supplementary Fig. 3C and 3D). In addition, the expression of ALP and Runx2 in H<sub>2</sub>S-deficient group was significantly lower than that in control group (Supplementary Fig. 3E

and 3F). These results confirmed that H<sub>2</sub>S does play a crucial role in regulating bone regeneration.

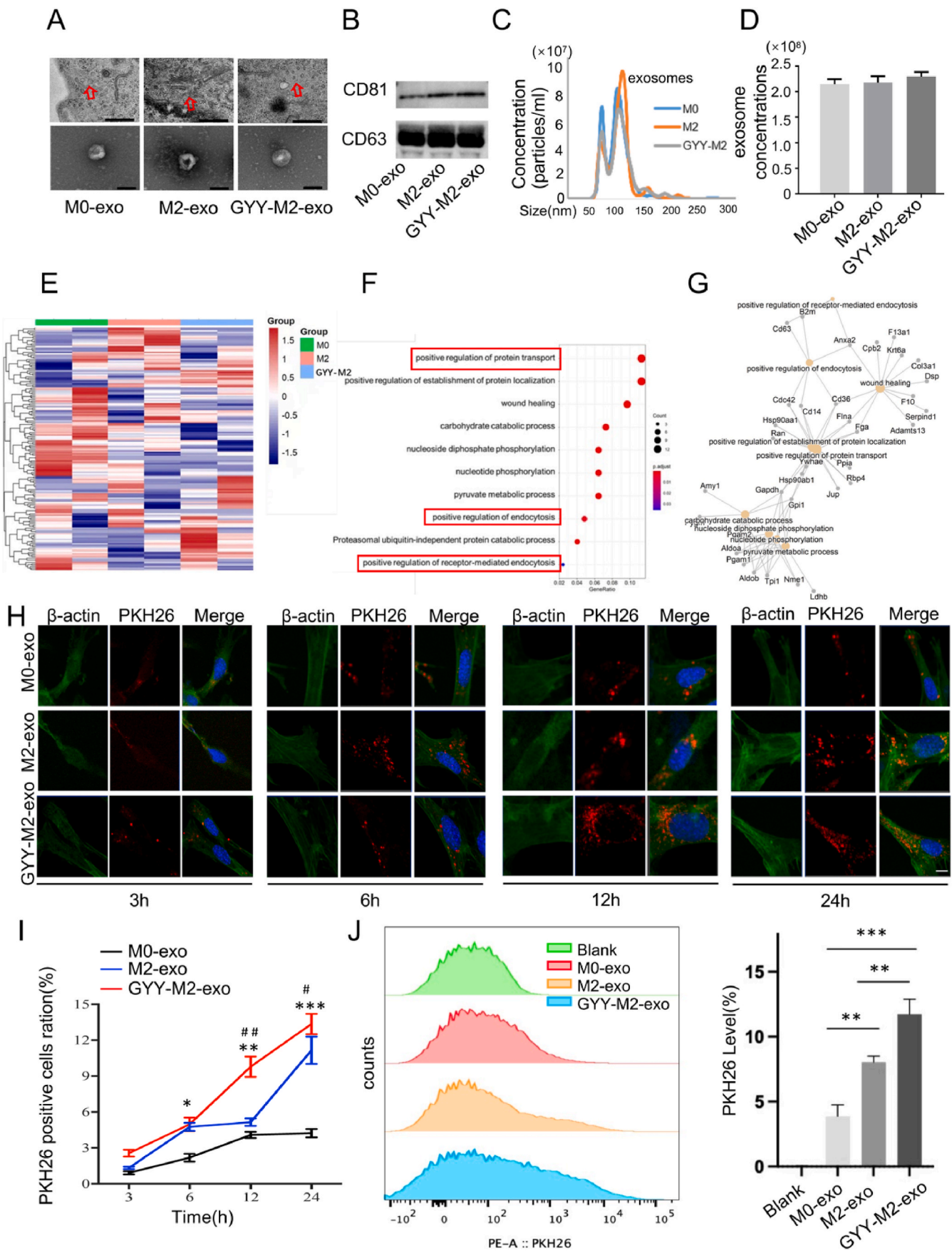
### 2.6. H<sub>2</sub>S promoted the enrichment of exosomal protein moesin

To explore how H<sub>2</sub>S regulates the exosomes property, we further analyzed the different proteins between M2 exosomes and H<sub>2</sub>S pretreated M2 exosomes by LC-MS analysis. The result showed that the moesin protein was one of the top-significantly enriched proteins in H<sub>2</sub>S pretreated-M2 exosomes compared with M2 exosomes (Fig. 6A). It is reported that moesin protein can affect the endocytosis of T cells and drosophila nephrocytes [21–23]. Then we found that H<sub>2</sub>S treatment promoted the expression of moesin both in macrophages and their exosomes (Fig. 6B and C). Furthermore, we used siRNA to knockdown the moesin in macrophages and found that the level of moesin protein was markedly reduced in siRNA treated macrophages and their exosomes (Fig. 6D). After moesin knocking down, the endocytosis of exosomes to MSCs was decreased observably (Fig. 6E). These results implied that H<sub>2</sub>S promoted the enrichment of moesin protein in macrophages exosomes to facilitate the endocytosis of exosomes by MSCs, thus to enhance osteogenic differentiation of MSCs.

### 2.7. Moesin protein in exosomes promoted the osteogenic differentiation of MSCs

It was reported that the moesin protein plays an important role in the early stage of osteoblast differentiation, and it can suppress breast cancer-associated bone loss [23]. To verify the role of exosomal protein moesin on bone regeneration, we used exosomes from moesin siRNA pretreated-macrophages. The results showed that the capacity of exosomes to promote bone regeneration of MSCs was inhibited after the





(caption on next page)

**Fig. 3. H<sub>2</sub>S treatment promoted exosomes endocytosis.** (A) Transmission electron microscope (TEM) image of exosomes purified from the culture supernatant from M0, M2 and H<sub>2</sub>S pretreated-M2 macrophages. (B) Western blot showed the protein expression of CD81 and CD63 in exosomes derived from M0, M2 and H<sub>2</sub>S pretreated-M2 macrophages. (C, D) The size (C) and quantity (D) of exosomes from M0, M2 and H<sub>2</sub>S pretreated-M2 macrophages were analyzed by Nanoparticle Tracking Analysis (NTA). (E) The protein profiles of exosomes derived from M0, M2 and H<sub>2</sub>S pretreated-M2 macrophages were analyzed LC-MS. The heat map showed the identified differential proteins. (F, G) The function of the different proteins was analyzed using Genn Ontology (GO) and Biological Process (BP) enrichment, and the results showed that the positive regulation of protein transport and positive regulation of endocytosis were among the top ten enriched clusters. (H, I) Immunofluorescent staining showed the endocytosis of M0 exosomes, M2 exosomes and H<sub>2</sub>S pretreated M2 exosomes by MSCs in a time course 3h, 6h, 12h and 24h. (J) The quantity analysis the ratio of MSCs which uptake the exosomes in blank, M0, M2 and H<sub>2</sub>S pretreated-M2 exosomes treatment groups by flow cytometry analysis. The exosomes were labeled with PKH26. Blank: BMSCs treated without exosomes. \* Compared with the M0 exosome group; # compared with M2 exosome group. Scale bars, 500 nm (upper panel) and 200 nm (lower panel, A), 5  $\mu$ m (I). Data are presented by mean  $\pm$  SD (\*P < 0.05, \*\*P < 0.01, \*\*\*P < 0.001).

moesin siRNA treatment, as determined by alizarin red S staining (Fig. 6F). The expression of osteogenic related-markers ALP and Runx2 also decreased in exosomes derived from moesin siRNA treatment group (Fig. 6G–J). Furthermore, we used recombinant moesin protein to treat MSCs and found that the osteogenic differentiation of MSCs increased after moesin protein treatment, as determined by ALP activity and Alizarin red staining (Fig. 6K, Supplementary Fig. 4). The expression of osteogenic related-markers ALP and Runx2 also increased after moesin protein treatment (Fig. 6L–N). These results indicated that the moesin protein is one of the mediators for M2 exosomes to promote bone regeneration.

### 2.8. Moesin activated $\beta$ -catenin signaling pathway in MSCs

The Wnt/ $\beta$ -catenin pathway plays an important role in bone regeneration [4]. Next, we investigated whether H<sub>2</sub>S pretreated-M2 exosomes can regulate the  $\beta$ -catenin signaling pathway to promote osteogenic differentiation of MSCs. We found that H<sub>2</sub>S pretreated-M2 exosomes promoted the expression of active- $\beta$ -catenin in MSCs (Fig. 7A). Conversely, exosomes derived from macrophages treated with moesin siRNA decreased the expression of active  $\beta$ -catenin in MSCs compared with the control exosomes treatment (Fig. 7B). Then, we treated MSCs with recombinant human moesin protein, and found that moesin protein promoted the expression of active  $\beta$ -catenin in MSCs. It has been reported that the phosphorylation of  $\beta$ -catenin is degraded through the ubiquitin-proteasome pathway [24]. We inhibited its biosynthesis and degradation by cycloheximide (CHX) and MG132 through ubiquitin-proteasome pathway, consequently discovered that moesin promoted the expression of active- $\beta$ -catenin by inhibiting p- $\beta$ -catenin (Fig. 7C). It has been described that active- $\beta$ -catenin is the form of  $\beta$ -catenin that enters the nucleus from the cytoplasm. Furthermore, we found that moesin promoted the nuclear translocation of active- $\beta$ -catenin (Fig. 7D). It showed that moesin inhibited the phosphorylation and degradation of  $\beta$ -catenin, thus promoting the expression of non-phosphorylated  $\beta$ -catenin and playing a further corresponding biological role in the nucleus. Moreover, the enhanced bone regeneration by moesin was attenuated by Wnt signaling inhibitor XAV-939 treatment (Fig. 7E–H, Supplementary Fig. 5A). In order to verify the role of  $\beta$ -catenin pathway in bone regeneration promoted by H<sub>2</sub>S pretreated-M2 exosomes, we pretreated MSCs with XAV-939 and the results showed that the capacity of M2 exosomes to promote bone regeneration was inhibited after XAV-939 treatment, as determined by ALP activity and alizarin red S staining. The expression of osteogenesis related markers ALP and Runx2 also decreased in the XAV-939 treatment group compared with the H<sub>2</sub>S pretreated-M2 exosomes treatment group. These results indicated that H<sub>2</sub>S pretreated-M2 exosomes promoted bone regeneration *via*  $\beta$ -catenin pathway (Supplementary Fig. 5B–5F). To analyze the effects of Wnt pathway on bone regeneration *in vivo*, we analyzed the expression of  $\beta$ -catenin using immunofluorescence staining. The results showed that M2 exosomes treatment could promote the number of active- $\beta$ -catenin positive cells. Moreover, the ratio of active- $\beta$ -catenin positive cells is significantly increased in H<sub>2</sub>S pretreated M2 exosomes group than the M2 exosomes group *in vivo* (Supplementary Fig. 5G). In order to verify the effects of Wnt pathway on bone regeneration, we used exosomes from H<sub>2</sub>S pretreated M2

macrophages to treat critical size calvarial bone defects in mice with or without XAV-939 administration. The results showed that M2 exosomes could significantly promote bone regeneration, which was attenuated by XAV-939 treatment, as assessed by Micro-CT and HE staining (Supplementary Fig. 5H and 5I). Moreover, the ratio of ALP and Runx2 positive cells, elevated by M2 exosomes treatment, was significantly decreased after XAV-939 administration (Supplementary Fig. 5J–5L). These results implied that Wnt pathway plays vital role in regulating bone regeneration. Conclusively, H<sub>2</sub>S pretreated exosomes possessed enriched moesin protein, which facilitates the exosome endocytosis by MSCs and enhances the osteogenic differentiation *via* activating  $\beta$ -catenin signaling (Fig. 7H).

### 3. Discussion

Recent studies have provided emerging evidence that H<sub>2</sub>S is an important regulator of macrophage polarization [15]. Our study found that H<sub>2</sub>S could promote macrophages towards M2 polarization, which is consistent with previous study [18]. However, 50  $\mu$ M H<sub>2</sub>S treatment failed to alter M1 polarization. It's reported that H<sub>2</sub>S produced by periodontal ligament stem cells activates M1 macrophages to promote orthodontic tooth movement *via* STAT1 signaling [25]. GYY4137 could also inhibit the LPS-induced M1 macrophage activation [26,27]. The role of H<sub>2</sub>S in M1 polarization may depend on the H<sub>2</sub>S concentration and processing time, and the exact effects still need further investigation.

M2 macrophages are responsible for the resolution of inflammation to enhance wound healing and tissue repair [8]. Inflammatory cytokines such as TNF- $\alpha$  and IFN- $\gamma$  dampen the capacity of MSCs is one of the main causes for the failure of bone regeneration [6]. The medium of M2 macrophages promoted the osteogenic differentiation of stem cells compared to the control group [20], suggesting the M2 macrophage may regulate MSCs property *via* paracrine pathway. Exosomes play a critical role in intercellular communication by transferring bioactive molecules between cells, such as lipids, proteins, and genetic information [28,29]. We found that the exosomes of M2 macrophages could induce osteogenic differentiation of MSCs, which is consistent with the previous study that exosomes of M2 macrophages induced MSCs to differentiate towards osteoblasts by targeting salt-inducible kinase 2 and 3 [30]. Moreover, M2 exosome treatment could enhance the local M2 macrophages to reestablish the immune microenvironment. While the M2 exosomes modified by the H<sub>2</sub>S treatment significantly promoted MSC-based calvarial bone regeneration more than M2 exosomes. Furthermore, we found that the exosomal protein moesin facilitated the endocytosis of exosomes into MSCs to activate- $\beta$ -catenin signaling, thus to promote osteogenic differentiation of MSCs and bone regeneration. It's reported that H<sub>2</sub>S could regulate a variety of cellular processes, such as NOX4-ROS signaling, NF- $\kappa$ B pathway, mitochondrial biogenesis and protein sulfhydration, and so on [16,18,31]. To our knowledge, this is the first time to report that H<sub>2</sub>S could regulate the exosomal protein profile in macrophages, without altering the exosome secretion and amounts. The exact mechanism of how H<sub>2</sub>S alter the exosomal proteins needs to be further investigated. It's reported that H<sub>2</sub>S could increase the self-renewal and osteogenic differentiation of MSCs and dental pulp stem cells through Wnt/ $\beta$ -catenin signaling [19,32]. These results indicated that H<sub>2</sub>S not only promoted osteogenic differentiation of stem cells

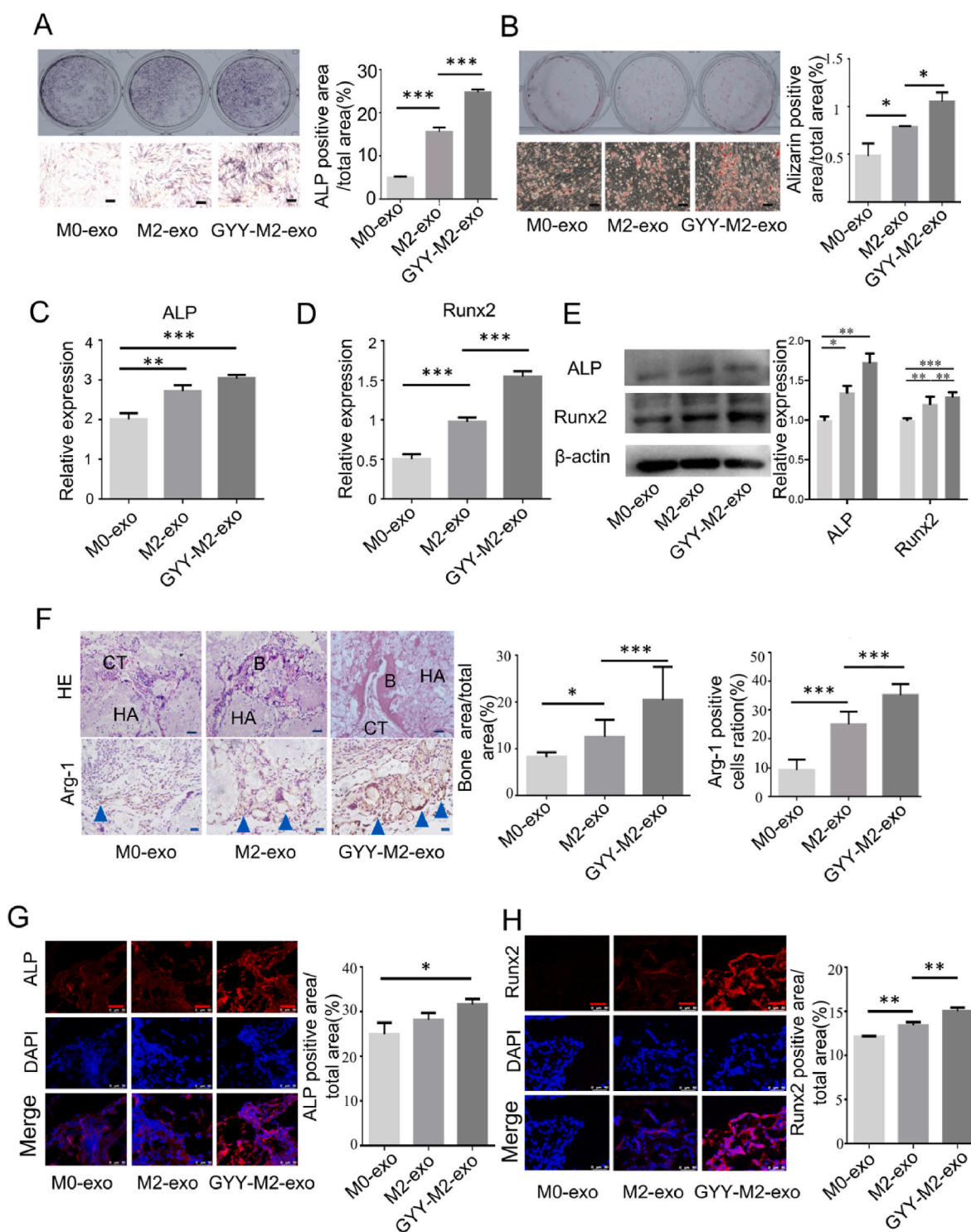


**Fig. 4.** The exosomes from H<sub>2</sub>S pretreated M2 macrophages promoted osteogenic differentiation of MSCs. (A) Alkaline phosphatase staining showed the ALP positive osteoblastic colonies in exosomes (50 µg/ml) from M0 macrophages, M2 macrophages and H<sub>2</sub>S pretreated-M2 macrophages treatment groups. (B) The mineralized nodule formation of MSCs treated by exosomes (50 µg/ml) from M0 macrophages, M2 macrophages and H<sub>2</sub>S pretreated-M2 macrophages treatment groups, as assessed by Alizarin red staining. (C–E) The expression of ALP and Runx2 of MSCs treated by exosomes from M0 macrophages, M2 macrophages and H<sub>2</sub>S pretreated-M2 macrophages treatment groups, as assessed by qPCR. (F) HE staining showed the bone formation of MSCs treated by exosomes (50 µg/ml) from M0 macrophages, M2 macrophages and H<sub>2</sub>S pretreated M2 macrophages treatment groups (upper panel). Immunohistochemical staining showed that the numbers of Arg-1 positive cells in exosomes from M0 macrophages, M2 macrophages and H<sub>2</sub>S pretreated-M2 macrophages treatment groups (lower panel). HA: hydroxyapatite; CT: connect tissue; B: bone. (G, H) Immunofluorescent staining showed the expression of ALP and Runx2. Scale bars, 100 µm. (F), 50 µm (G–H). Data are presented by mean ± SD (\*P < 0.05, \*\*P < 0.01, \*\*\*p < 0.001).



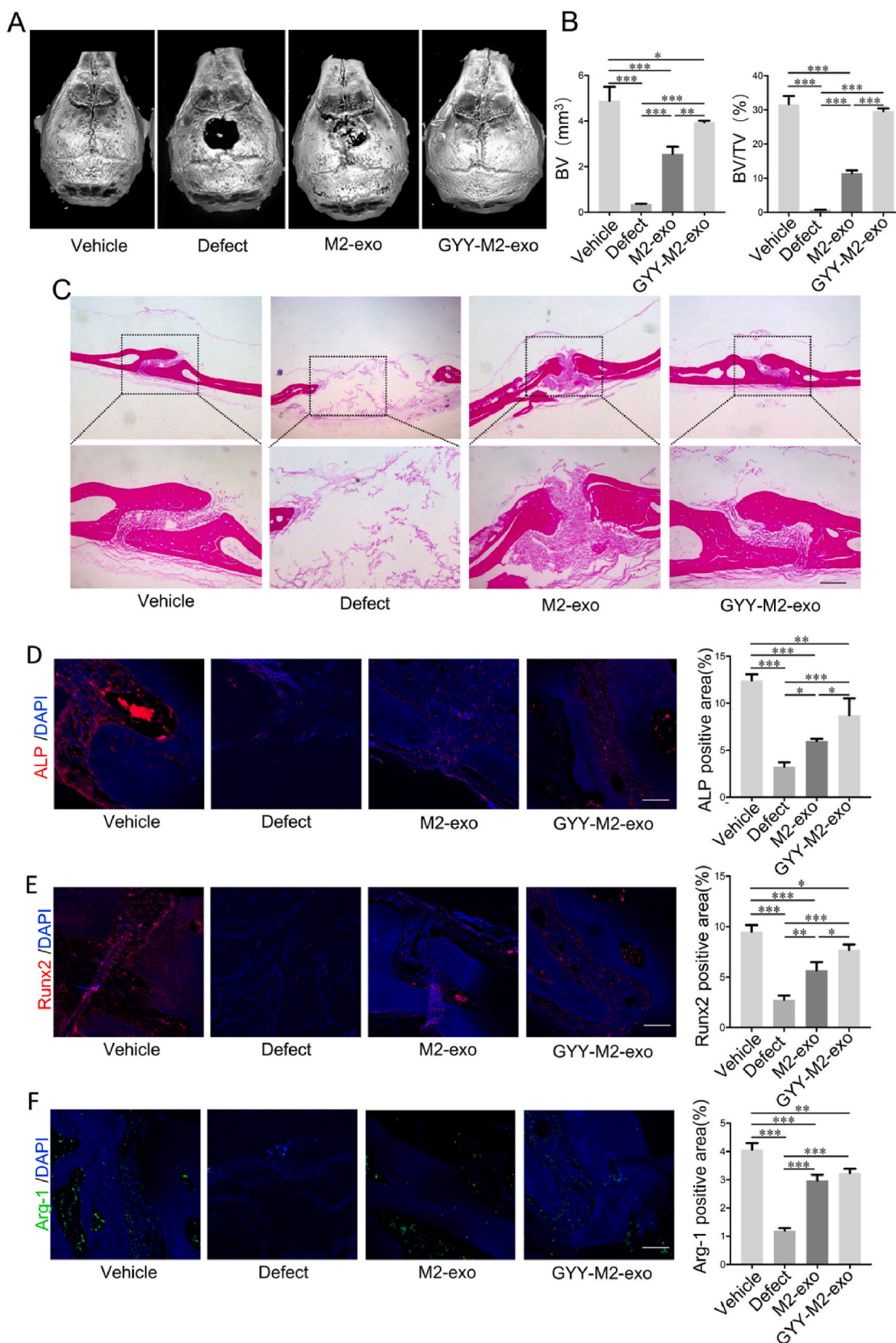


**Fig. 5.** M2 exosomes modified by H<sub>2</sub>S enhanced calvarial bone defects regeneration. (A, B) The calvarial bone morphology in vehicle, bone defect, M2 exosomes and H<sub>2</sub>S modified M2 exosomes (200 μg) treatment groups analyzed by micro-CT. BV: bone volume; BV/TV: bone volume/total volume. (C) The calvarial bone tissue structure in vehicle, defect, M2 exosomes and H<sub>2</sub>S modified M2 exosomes treatment groups, as assessed by HE staining. (D–F) The enrichment of ALP, Runx2 and Arg-1 positive cells in bone regeneration area of vehicle, defect and M2 exosomes and H<sub>2</sub>S modified M2 exosomes treatment groups, as assessed by Immunofluorescent staining. Scale bars, 100 μm (C), 50 μm (D–F). Data are presented by mean ± SD (\*P < 0.05, \*\*P < 0.01, \*\*\*p < 0.001).



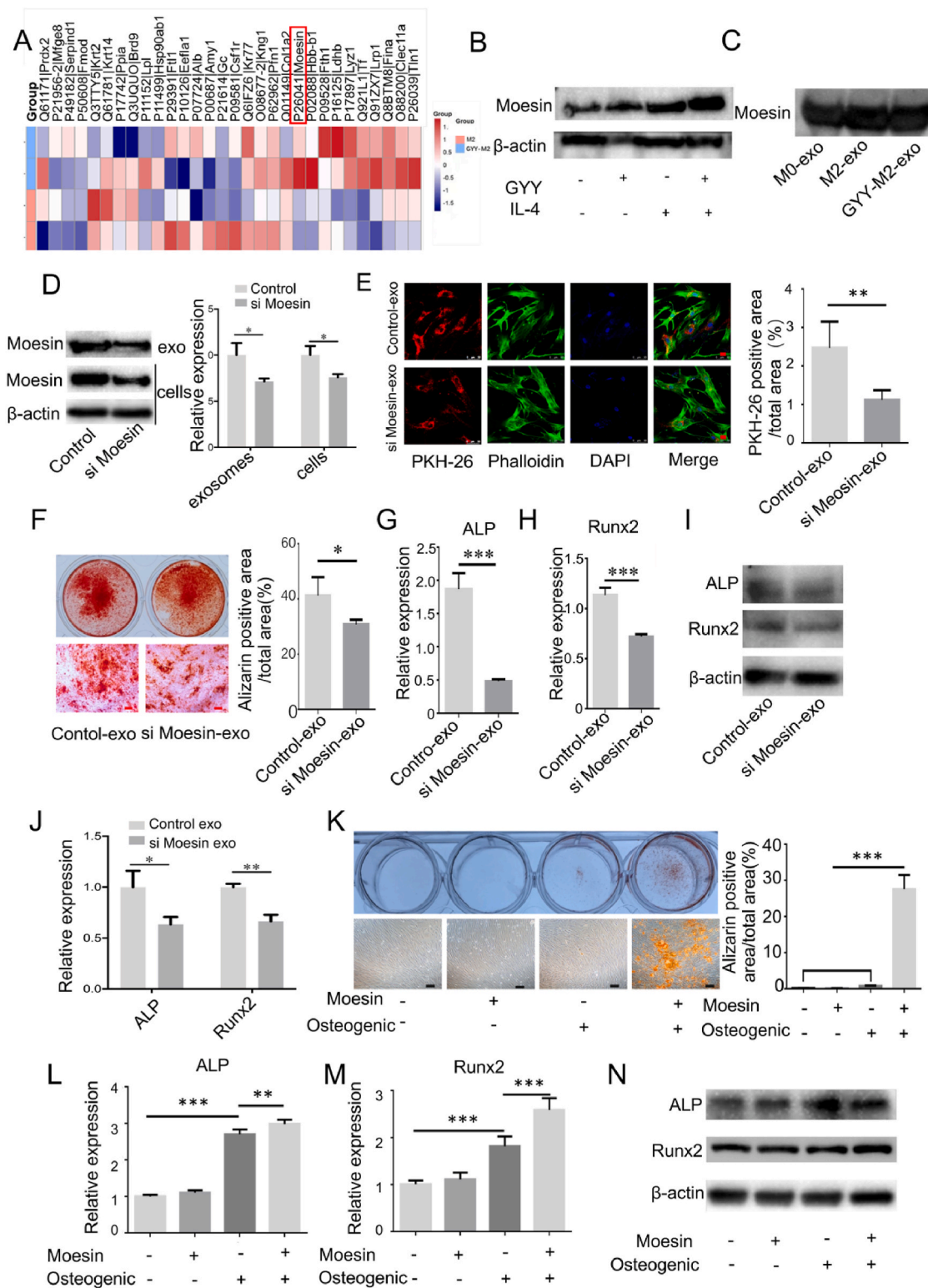


**Fig. 6.** H<sub>2</sub>S modified M2 exosomes promoted osteogenic differentiation of MSCs via moesin mediated endocytosis. (A) The top 30 significantly different proteins between M2 exosomes and H<sub>2</sub>S pretreated M2 exosomes. (B) The expression of moesin in M0, M2 and H<sub>2</sub>S pretreated-M2 macrophages, as assessed by western blot. (C) The expression of moesin in exosomes derived from M0, M2 and H<sub>2</sub>S pretreated-M2 macrophages, as assessed by western blot. (D) The expression of meosin in macrophages and exosomes, with or without moesin siRNA treatment. (E) Immunofluorescent staining showed the endocytosis of exosomes from macrophages treated with or without moesin siRNA. (F) The mineralized nodule formation of MSCs stimulated by control or moesin siRNA pretreated-exosomes. (G–J) The expression of ALP and Runx2 of MSCs stimulated by control or moesin siRNA pretreated-exosomes, as assessed by qPCR analysis and western blot. (K) The mineralized nodule formation of MSCs treated with or without moesin protein (5 μg/ml). (L–N)The expression of ALP and Runx2 of MSCs treated with or without moesin protein, as assessed by qPCR and western blot analysis. Scale bars: 10 μm (E), 50 μm (F, K). Data are presented by mean ± SD (\*P < 0.05, \*\*P < 0.01, \*\*\*P < 0.001).

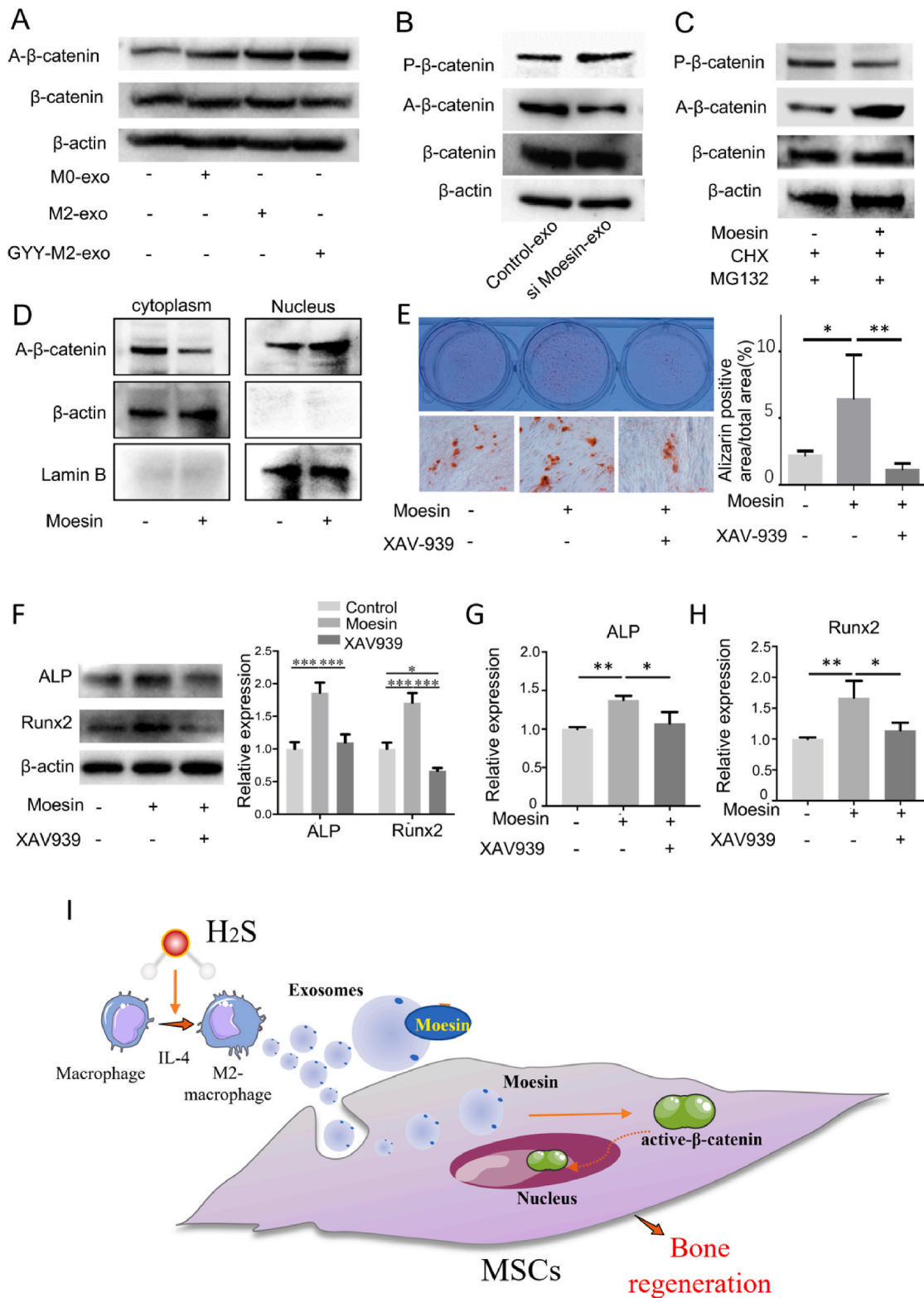


**Fig. 7.** H<sub>2</sub>S modified M2 exosomes promoted osteogenic differentiation of MSCs through β-catenin signaling pathway. (A) The expression of β-catenin and active β-catenin in control MSCs, MSCs treated by exosomes derived from M0, M2 and H<sub>2</sub>S pretreated-M2 macrophages, as assessed by western blot. (B) The expression of β-catenin and active β-catenin in control MSCs or moesin siRNA pretreated-exosomes treated MSCs. (C) The protein levels of p-β-catenin, active-β-catenin, and β-catenin in control and moesin groups treatment with CHX (20 μg/mL) for 10h, then with MG132 (10 μmol/L) for 2h. (D) The expression of active-β-catenin in the cell cytoplasm and nucleus fraction with or without moesin treatment. (E) The mineralized nodule formation in control, stimulated by moesin with or without XAV-939 (3 μM) treatment groups. (F–H) The expression of ALP and Runx2 of MSCs in control, stimulated by moesin with or without XAV-939 treatment groups, as assessed by qPCR analysis and western blot. (I) The schema showed that H<sub>2</sub>S promoted M2 macrophages polarization with enhancing the level of exosomal protein moesin, which facilitated the uptake of exosomes by MSCs. Thus, the exosomes, from H<sub>2</sub>S pretreated M2 macrophages, promoted bone regeneration of MSCs via activating β-catenin signaling pathway. Scale bars: 50 μm Data are presented by mean ± SD (\*P < 0.05, \*\*P < 0.01, \*\*\*P < 0.001).

directly but also provided a microenvironment friendly to bone regeneration indirectly via promoting M2 macrophage polarization.

The unique property of H<sub>2</sub>S signals is mediated by the sulfhydrylation of proteins [33]. Protein S-sulfhydrylation participates and regulates the processes of cell survival/death, cell differentiation, cell proliferation, mitochondrial bioenergetics/biogenesis, endoplasmic reticulum stress, inflammation, and oxidative stress et al. [34]. Sulfhydrylation occurs at reactive cysteine residues in proteins and results in the conversion of an –SH group of cysteine to an –SSH or a persulfide group. Sulfhydrylation is highly prevalent *in vivo*, and aberrant sulfhydrylation patterns have been observed under several pathological conditions ranging from heart disease to neurodegenerative diseases [35]. Studies have shown that sulfhydrylation is involved in the regulation of protein vesicle-associated membrane protein 3 (VAMP3), which takes part in exosome release [36]. However, whether H<sub>2</sub>S signals mediated sulfhydrylation regulating exosomes generation or release need to be further studied.

Moesin protein is a member of the Ezrin Radixin moesin (ERM) family, which is mainly distributed in the surface structure of actin-rich cells and crosslinks actin filaments with the plasma membrane. Moesin is not only involved in cytoskeleton organization such as the formation of microvilli, cell-cell adhesion, cell motility and membrane trafficking but also is involved in the regulation of various signal pathways such as Rho pathway and PI3-kinase/Akt pathway [37]. Moesin could suppress breast cancer-associated bone loss *via* inhibition of TGFβ/FN1/CD44 signaling [38]. Moesin controls clathrin-mediated S1PR1 endocytosis in T Cells [21]. Here, we found that H<sub>2</sub>S treatment alters the protein profile of exosomes derived from M2 macrophages. The moesin protein is one of the significantly highly enriched proteins. Moreover, the enriched moesin in the exosomes from M2 macrophages could promote the endocytosis of exosomes into MSCs, while the amounts of exosomes trafficked into MSCs were significantly decreased after the moesin was decreased by siRNA pretreatment. Our results indicated that moesin takes part in the uptake of exosomes. Several proteins have been identified as participants in the endocytosis of exosomes such as Cadherin 11, CD9, CD81, and Integrin α6β4 [39]. To our knowledge, this is the first time to report that moesin is linked to vesicle internalization to promote osteogenic differentiation of MSCs. However, the specific mechanism needs further investigation. Research into internalization mechanisms has shown that the experimental manipulation of the exosomal membrane protein profile, such as stripping the membrane, affects the uptake of exosomes [40,41]. This endocytosis process is inverted with the cargo release, which was mainly mediated by the endosomal sorting complex required for transport (ESCRT) [42]. ESCRT machinery mediates various membrane scission events within cells and seems to be dedicated to scission of small cytosol-containing double-membrane openings [43]. In this study, we found that H<sub>2</sub>S failed to alter the release of exosomes, including the quantity and size of the exosomes and the expression of CD63 and CD81, but increased the enrichment of moesin protein in exosomes, which increased the exosome endocytosis to regulate bone regeneration. These results indicated that moesin may play a role in endocytosis, but not in the ESCRT independent exosome release. However, the exact role of moesin on cargo release and transport needs to be further investigated.

It was found that moesin is a glioma progression marker that induces proliferation and Wnt/β-catenin pathway activation *via* interaction with CD44 [44]. Our results showed that moesin could also increase the osteogenic differentiation of MSCs by activating Wnt/β-catenin signaling. A variety of signaling, such as Notch signaling [45], TGF-β and BMP signaling [23,46], take part in MSC-based bone regeneration. Whether or not moesin regulates other signaling pathways linked with bone regeneration needs more in-depth research.

In summary, we found that H<sub>2</sub>S promoted M2 macrophage polarization by manipulating the protein profile of exosomes from M2 macrophages. The enriched M2 macrophage exosomal protein moesin facilitated the uptake of exosomes by MSCs to enhance MSC bone regeneration through β-catenin signaling. This study provides a new

strategy to modify exosomes to promote bone regeneration and tissue engineering.

## 4. Materials and methods

### 4.1. Cells culture and treatment

Murine macrophage RAW 264.7 cells were purchased from National Infrastructure of Cell Line Resource (Beijing, China) and cultured with RPMI 1640 medium containing 10% FBS and 1% penicillin/streptomycin at 37 °C with 5% CO<sub>2</sub>. For M1 polarization, RAW 264.7 were seeded in 6-well dishes at a density of 5 × 10<sup>5</sup> cells per well, and then were treated with 1 μg/ml LPS (Sigma, American), combined with or without 50 μM H<sub>2</sub>S donor (GYY 4137, Abcam, American) treatment for 24h. For the M2 polarization, RAW 264.7 were treated by 50 ng/ml IL-4 (Peprotech, American), with or without 50 μM H<sub>2</sub>S donor GYY 4137 treatment for 24h. For the inhibition of moesin, the RAW 264.7 were pretreated with 1 μg siRNA of moesin (Santa Cruz Biotechnology, American) for 24h.

Human bone marrow stem cells were purchased from Science Cell (American) and cultured with α-MEM medium containing 15% FBS and 1% penicillin/streptomycin at 37 °C with 5% CO<sub>2</sub>. The passage 2 to passage 5 of MSCs were used for further investigation.

### 4.2. Osteogenic differentiation assay

For osteogenic differentiation, MSCs were seeded in 6-well dishes at a density of 5 × 10<sup>5</sup> cells per well, and treated with osteogenic differentiation medium (α-MEM medium containing 15% FBS, 1% penicillin/streptomycin and 50 μg/mL ascorbic acid), macrophage culture conditional medium, 50 μg/ml different exosomes, or 5 μg/ml moesin protein (aa 1–346, His Tag, Sino Biological, China).

For macrophage conditional medium preparation, RAW264.7, 70–80% confluent, were cultured with 1640 medium containing 10% RPMI 1640 medium containing 10% FBS and 1% penicillin/streptomycin with or without 50 μM GYY 4137 treatment. The macrophage culture medium was collected after 48 h by centrifuging for 5 min at 400 g. Then the supernatant was centrifuged again at 5000 g for 20 min to remove cell debris, followed by filtered at 0.22 μm, and then stored at –80 °C until use. The conditioned medium for osteogenic induction were prepared by mixing macrophage culture medium with to osteogenic medium at the ratio of 1:3. For the control group, the 1640 medium mixed with osteogenic medium (1:3).

For ALP staining, after 7 days osteogenic induction, the cells were fixed in 4% PFA and stained with alkaline phosphatase (Solarbio, China) at room temperature. For Alizarin red staining, after 21 days osteogenic induction, the cells were fixed in 4% PFA and stained with 1% Alizarin Red S (Solarbio, China) at room temperature. The ALP/Alizarin Red-positive area was measured by Image J software and expressed as the percentage of ALP/Alizarin Red-positive area over the total area.

### 4.3. Isolation, analysis and labeling of exosomes

Exosomes were isolated from M0, M2 and GYY4137 pretreated-M2 macrophages. The macrophages were cultured in 1640 with exosome-free serum (centrifuged at 120,000g for 90 min) for 24h. The culture supernatant was collected and exosomes were isolated by ultracentrifugation according to previously described standard methods [47]. Optima MAX-XP (Beckman Coulter, USA) was used to perform ultracentrifugation experiments. The final exosomes were resuspended in PBS for further analysis. Using bicinchoninic acid to assay the protein amounts of exosomes. Transmission electron microscope (TEM, JEM-1400PLUS, Japan) was performed to observe exosomes. Nanoparticle tracking analysis (NTA) was performed at Shanghai Biotechnology Corporation (Shanghai, China) with the ZetaView PMX 110 (Malvern Instruments Ltd, UK) to quantify exosomes. PKH-26 (Sigma,



Aldrich, USA) was used for exosome labeling according to the instructions of the manufacturer. For extraction of exosomes protein, the extracted exosomes were added with RIPA lysate containing 1% protease inhibitor and mixed evenly in EP tube. After standing at room temperature for 5 min, intermixture was centrifuged at 12000g at 4 °C for 25 min. Supernatant was transferred to a newly labeled EP tube.

#### 4.4. Transmission electron microscopy (TEM)

Exosomes were fixed in 2% paraformaldehyde, washed, and loaded onto Formvar-carbon-coated grids. After washing, exosomes were postfixated in 2% glutaraldehyde for 2 min, washed, and contrasted with 2% phosphotungstic acid for 5 min. Samples were washed, dried, and examined by an electron microscope (JEM-1400PLUS, Japan).

For cells, different macrophages were fixed with 2.5% glutaraldehyde overnight and then fixed with 1% osmium tetroxide for 2 h, dehydrated in a graded series of ethanol concentrations, and embedded in SPIPON812 resin and polymerized. The block was sectioned by microtome (Leica EM UC6). The ultrathin sections approximately 70 nm, mounted on copper grids, uranyl acetate, and lead citrate were used to stain, examined, and photographed with an FEI Tecnai spirit TEM (FEI Tecnai Spirit 120 kv).

#### 4.5. Nanoparticle tracking analysis (NTA)

NTA was performed with the ZetaView PMX 110 (Particle Metrix, Meerbusch, Germany). In order to measure the particle size and concentration, purified exosomes were diluted with PBS buffer. ZetaView 8.04.02 software was used to analyze the data. To convert the yield from concentration to associate degree correct range of particles, dilution factors and suspension volumes were used.

#### 4.6. Western blot analysis

Cells and exosomes were lysed by a macromolecule extraction kit (RIPA Cocktail, Thermo). Nucl-Cyto-Mem Preparation Kit was purchased from Applygen (Beijing, China). SDS-PAGE was applied to isolate constant quantity of proteins, thus the proteins were transferred onto a polyvinylidene halide membrane. The membranes were blocked with 5% non-fat milk and 0.1% Tween-20 for 1 h and incubated with CD63 (1:1,000, Abclonal Technology), CD81 (1:500),  $\beta$ -actin (1:10000) (Santa Cruz Biotechnology), Moesin (1:1000, Abcam),  $\beta$ -catenin, active- $\beta$ -catenin (1:1000, Santa Cruz Biotechnology) primary antibodies at 4 °C overnight. Blots were incubated by HRP-conjugated secondary protein for 1 h and subjected to increased luminescence detection. Qualitative analysis was performed by the ImageLab package provided by the manufacturer (Bio-Rad).

#### 4.7. Immunofluorescence staining

Cells were fixed in 4% paraformaldehyde and washed with PBS. Then the cells were stained by primary antibodies of iNOS (1:200, Cell signaling Technology) and Arg-1 (1:200, Cell signaling Technology). MSCs with or without PKH26-exosomes were stained with Fluorescently-labeled phalloidin (Green, Invitrogen, USA). Nuclei were counterstained with 4',6-diamidino-2-phenylindole. Confocal microscopic pictures were processed with LSM five unharness four, when acquired by a laser-scanning magnifier (LSM 510, Zeiss).

#### 4.8. Protein identification using mass spectrometry

For proteomic analysis of exosomes, exosome samples were lysed by sodium dodecyl sulfate. 5  $\mu$ g of exosome proteins per group were isolated using SDS-PAGE gel followed by coomassie blue staining and destaining. The whole lane corresponding to each sample was cut into 1

mm  $\times$  1 mm cube by using a clean scalpel. Then the gels were destained, reduced with dithiothreitol solution (5 mM dithiothreitol in 50 mM ammonium bicarbonate), alkylated with iodoacetamide solution (11 mM iodoacetamide in 50 mM ammonium bicarbonate). Then trypsin solution was added into gels for digestion overnight at 37 °C. The supernatant containing the digested peptides was transferred into a clean tube for LC-MS/MS analysis. The raw data of mass spectrometry was searched against the uniprot proteome of human by using the Proteome Discoverer software (version 1.4, Thermo Scientific). The parameters for database searching were static modifications of carbamidomethylation (+57.021 Da) on cysteine; dynamic modification of oxidation (+15.995 Da) on methionine; no more than two missed cleavages were allowed; the mass tolerances of precursors and fragments were 20 ppm and 0.02 Da, respectively; only peptides with false discovery rate below 1% were considered as high-confidence hits; only unique peptides were used for protein quantification.

#### 4.9. Measurement of H<sub>2</sub>S levels

The H<sub>2</sub>S levels in macrophage culture medium were analyzed by using the free radical analyzer TBR4100 with an H<sub>2</sub>S-selective sensor (ISO-H<sub>2</sub>S-100, WPI, China). Firstly, the calibration curve with a plot of the signal output (pA)-H<sub>2</sub>S concentration was generated by PBS buffer containing different concentrations of Na<sub>2</sub>S using the sensor tip. Then, the sensor tip was used to analyze the H<sub>2</sub>S concentration in every sample according to the calibration curve.

#### 4.10. Mouse MSCs implantation

Following the Animal Use and Care Committee of Beijing University approval (LA2022022), 8-wk-old nude mice (male, 20–25g) (Vitalriver, Beijing, China) were employed in our study. Hydroxyapatite/tricalcium phosphate (HA/TCP) ceramic powders (40 mg; framing, Inc.) were mixed with  $4 \times 10^6$  MSCs (MSCs treated with 50  $\mu$ g exosomes from M0, M2 and GYY4137 pretreated-M2 macrophages for 48 h, respectively) and subcutaneously transplanted into the dorsal surface of eight-week-old nude mice for 8 weeks (n = 4). At eight weeks post-transplantation, the implants were harvested, fastened in four-dimensional PFA, then decalcified with five-hitter ethylenediaminetetraacetic acid (EDTA; pH 7.4), followed by paraffin embedding.

#### 4.11. Calvarial bone defects assay

To analyze the effect of exosomes on calvarial bone defects, 3  $\times$  3 mm critical bone defects were established on calvarial bones of C57BL6 mice (n = 4). 200  $\mu$ g exosomes from M2 and GYY4137 pretreated-M2 macrophages were mixed with 200  $\mu$ l Matrigel (Corning, 8015323), respectively. The Matrigel with exosomes were transplanted to newly generated calvarial bone defects. Then the gelfoam were used to cover previous implanted exosomes Matrigel complex in the calvarial bone defect area. No exosomes were added in control group. Then the calvarial bone defects were completely covered with skin and sutured. At eight weeks post bone defects, the samples of the calvarial bone were collected for further analysis. To investigate the effect of wnt signaling on bone regeneration, the mice were injected the inhibitors (XAV-939) or DMSO *via* intraperitoneal injection 1 day before the exosomes administration. And XAV-939 was injected every other day for 2 weeks (10 mg/kg per injection). DMSO (10%) diluted in saline was used as a control and to dissolve the inhibitors (XAV-939).

To analyze the role of endogenous H<sub>2</sub>S on bone regeneration, 2.5  $\times$  2.5 mm bone defects were established on calvarial bones of control and *Cbs*<sup>-/-</sup> (B6.129P2-Cbstm1Unc/J, JAX #002461) mice (n = 4) [31]. Eight weeks after bone defects, the samples of the calvarial bone were collected for further analysis.



#### 4.12. Immunohistochemical staining and hematoxylin and eosin (HE) staining

Briefly, the assay was performed with a ballroom dance detection kit (Zhongshan Golden Bridge Biotechnology, Beijing, China) as the instruction described. The ultimate result came from the common of 3 tests.

#### 4.13. Real-time polymerase chain reaction (qPCR)

Total polymer of the treated cells was extracted by TRIZOL chemical agent (Invitrogen, USA) and synthesis of desoxyribonucleic acid was performed with the SuperScript RT-PCR System (Thermo Fisher Scientific, Rockford, IL, USA) with Pt Taq hi-fi (Invitrogen, USA). Quantitative RT-PCR was performed on a period PCR System (Applied Biosystems 7500, USA) using 2 × SYBR green (Invitrogen Life Technologies, USA). The subsequent primers were used as the appendix table. The amplification specificity of the freshly designed primers was confirmed by melting curve. Potency was confirmed by sequencing standard PCR products.

#### 4.14. Statistical analysis

Statistical analysis was performed by SPSS 19 software. Independent unpaired two-tailed Student's *t* tests were used to analyze the comparisons between 2 groups. One-way analysis of variance (ANOVA) was used to analyze the comparisons among more than 2 groups. *P* values < 0.05 were considered statistically significant.

#### Funding

This work was supported by the National Science and Technology Major Project of the Ministry of Science and Technology of China No. 2022YFA1105800, the National Natural Science Foundation of China No. 81970940 (R.Y), and Ten-thousand Talents Program QNBJ-2020(R.Y).

#### Acknowledgements

We thank the Facility for Protein Chemistry and Proteomics of Tsinghua University for the exosome proteomic profile analysis by LC-MS. We appreciate the assist from Dr. Hongfang Jin in Department of Pediatrics, Peking University First Hospital for the measurement of H<sub>2</sub>S level.

#### Appendix A. Supplementary data

Supplementary data to this article can be found online at <https://doi.org/10.1016/j.bioactmat.2023.08.006>.

#### References

- R. Wang, The gasotransmitter role of hydrogen sulfide, *Antioxidants Redox Signal.* 5 (2003) 493–501, <https://doi.org/10.1089/152308603768295249>.
- T. Xiao, Z. Yan, S. Xiao, Y. Xia, Proinflammatory cytokines regulate epidermal stem cells in wound epithelialization, *Stem Cell Res. Ther.* 11 (2020) 232, <https://doi.org/10.1186/s13287-020-01755-y>.
- Y. Li, D. Zhang, L. Xu, L. Dong, J. Zheng, Y. Lin, J. Huang, Y. Zhang, Y. Tao, X. Zang, D. Li, M. Du, Cell-cell contact with proinflammatory macrophages enhances the immunotherapeutic effect of mesenchymal stem cells in two abortion models, *Cell. Mol. Immunol.* 16 (2019) 908–920, <https://doi.org/10.1038/s41423-019-0204-6>.
- Z. Huang, X. Pei, D.T. Graves, The interrelationship between diabetes, IL-17 and bone loss, *Curr. Osteoporos. Rep.* 18 (2020) 23–31, <https://doi.org/10.1007/s11914-020-00559-6>.
- T. Ono, H. Takayanagi, Osteoimmunology in bone fracture healing, *Curr. Osteoporos. Rep.* 15 (2017) 367–375, <https://doi.org/10.1007/s11914-017-0381-0>.
- Y. Liu, L. Wang, T. Kikuri, K. Akiyama, C. Chen, X. Xu, R. Yang, W. Chen, S. Wang, S. Shi, Mesenchymal stem cell-based tissue regeneration is governed by recipient T lymphocytes via IFN- $\gamma$  and TNF- $\alpha$ , *Nat. Med.* 17 (2011) 1594–1601, <https://doi.org/10.1038/nm.2542>.
- D.F. Kinane, P.G. Stathopoulou, P.N. Papapanou, Periodontal diseases, *Nat. Rev. Dis. Prim.* 3 (2017), 17038, <https://doi.org/10.1038/nrdp.2017.38>.
- C. Schlundt, T. El Khassawna, A. Serra, A. Dienelt, S. Wendler, H. Schell, N. van Rooijen, A. Radbruch, R. Lucius, S. Hartmann, G.N. Duda, K. Schmidt-Bleek, Macrophages in bone fracture healing: their essential role in endochondral ossification, *Bone* 106 (2018) 78–89, <https://doi.org/10.1016/j.bone.2015.10.019>.
- M. Kurowska-Stolarska, B. Stolarski, P. Kewin, G. Murphy, C.J. Corrigan, S. Ying, N. Pitman, A. Mirchandani, B. Rana, N. van Rooijen, M. Shepherd, C. McSharry, I. B. McInnes, D. Xu, F.Y. Liew, IL-33 amplifies the polarization of alternatively activated macrophages that contribute to airway inflammation, *J. Immunol.* 183 (2009) 6469–6477, <https://doi.org/10.4049/jimmunol.0901575>.
- A. Shapouri-Moghaddam, S. Mohammadian, H. Vazini, M. Taghadosi, S.-A. Esmaeili, F. Mardani, B. Seifi, A. Mohammadi, J.T. Afshari, A. Sahebkar, Macrophage plasticity, polarization, and function in health and disease, *J. Cell. Physiol.* 233 (2018) 6425–6440, <https://doi.org/10.1002/jcp.26429>.
- A. Golchin, S. Hosseinzadeh, A. Ardeshiryajimi, The exosomes released from different cell types and their effects in wound healing, *J. Cell. Biochem.* 119 (2018) 5043–5052, <https://doi.org/10.1002/jcb.26706>.
- M. Kang, C.-C. Huang, Y. Lu, S. Shirazi, P. Gajendradreddy, S. Ravindran, L. F. Cooper, Bone regeneration is mediated by macrophage extracellular vesicles, *Bone* 141 (2020), 115627, <https://doi.org/10.1016/j.bone.2020.115627>.
- C. Szabo, A timeline of hydrogen sulfide (H<sub>2</sub>S) research: from environmental toxin to biological mediator, *Biochem. Pharmacol.* 149 (2018) 5–19, <https://doi.org/10.1016/j.bcp.2017.09.010>.
- N. Dilek, A. Papapetropoulos, T. Toliver-Kinsky, C. Szabo, Hydrogen sulfide: an endogenous regulator of the immune system, *Pharmacol. Res.* 161 (2020), 105119, <https://doi.org/10.1016/j.phrs.2020.105119>.
- F. Sun, J.-H. Luo, T.-T. Yue, F.-X. Wang, C.-L. Yang, S. Zhang, X.-Q. Wang, C.-Y. Wang, The role of hydrogen sulphide signalling in macrophage activation, *Immunology* 162 (2021) 3–10, <https://doi.org/10.1111/imm.13253>.
- X.-L. Wang, L.-L. Pan, F. Long, W.-J. Wu, D. Yan, P. Xu, S.-Y. Liu, M. Qin, W.-W. Jia, X.-H. Liu, Y.Z. Zu, Endogenous hydrogen sulfide ameliorates NOX4 induced oxidative stress in LPS-stimulated macrophages and mice, *Cell. Physiol. Biochem.* 47 (2018) 458–474, <https://doi.org/10.1159/000489980>.
- L. Li, M. Salto-Tellez, C.-H. Tan, M. Whiteman, P.K. Moore, GYY4137, a novel hydrogen sulfide-releasing molecule, protects against endotoxic shock in the rat, *Free Radic. Biol. Med.* 47 (2009) 103–113, <https://doi.org/10.1016/j.freeradbiomed.2009.04.014>.
- L. Miao, X. Shen, M. Whiteman, H. Xin, Y. Shen, X. Xin, P.K. Moore, Y.-Z. Zhu, Hydrogen sulfide mitigates myocardial infarction via promotion of mitochondrial biogenesis-dependent M2 polarization of macrophages, *Antioxidants Redox Signal.* 25 (2016) 268–281, <https://doi.org/10.1089/ars.2015.6577>.
- Y. Liu, R. Yang, X. Liu, Y. Zhou, C. Qu, T. Kikuri, S. Wang, E. Zandi, J. Du, I. S. Ambudkar, S. Shi, Hydrogen sulfide maintains mesenchymal stem cell function and bone homeostasis via regulation of Ca<sup>2+</sup> channel sulfhydration, *Cell Stem Cell* 15 (2014) 66–78, <https://doi.org/10.1016/j.stem.2014.03.005>.
- S. Chen, H. Liang, Y. Ji, H. Kou, C. Zhang, G. Shang, C. Shang, Z. Song, L. Yang, L. Liu, Y. Wang, H. Liu, Curcumin modulates the crosstalk between macrophages and bone mesenchymal stem cells to ameliorate osteogenesis, *Front. Cell Dev. Biol.* 9 (2021), 634650, <https://doi.org/10.3389/fcell.2021.634650>.
- A. Nomachi, M. Yoshinaga, J. Liu, P. Kanchanawong, K. Tohyama, D. Thumkeo, T. Watanabe, S. Narumiya, T. Hirata, Moesin controls clathrin-mediated S1PR1 internalization in T cells, *PLoS One* 8 (2013), e82590, <https://doi.org/10.1371/journal.pone.0082590>.
- F. Hochapfel, L. Denk, G. Mendl, U. Schulze, C. Maaßen, Y. Zaytseva, H. Pavenstädt, T. Weide, R. Rachel, R. Witzgall, M.P. Krahn, Distinct functions of Crumbs regulating slit diaphragms and endocytosis in *Drosophila* nephrocytes, *Cell. Mol. Life Sci.* 74 (2017) 4573–4586, <https://doi.org/10.1007/s00018-017-2593-y>.
- D. Hong, H.-X. Chen, H.-Q. Yu, Y. Liang, C. Wang, Q.-Q. Lian, H.-T. Deng, R.-S. Ge, Morphological and proteomic analysis of early stage of osteoblast differentiation in osteoblastic progenitor cells, *Exp. Cell Res.* 316 (2010) 2291–2300, <https://doi.org/10.1016/j.yexcr.2010.05.011>.
- S.J. S.C. Weiss, A. Clerk, Glycogen synthase kinase 3 (GSK3) in the heart: a point of integration in hypertrophic signalling and a therapeutic target? A critical analysis, *Br. J. Pharmacol.* 153 (Suppl 1) (2008) S137–S153, <https://doi.org/10.1038/sj.bjp.0707659>.
- D. He, F. Liu, S. Cui, N. Jiang, H. Yu, Y. Zhou, Y. Liu, X. Kou, Mechanical load-induced H<sub>2</sub>S production by periodontal ligament stem cells activates M1 macrophages to promote bone remodeling and tooth movement via STAT1, *Stem Cell Res. Ther.* 11 (2020) 112, <https://doi.org/10.1186/s13287-020-01607-9>.
- L. Li, M. Salto-Tellez, C.-H. Tan, M. Whiteman, P.K. Moore, GYY4137, a novel hydrogen sulfide-releasing molecule, protects against endotoxic shock in the rat, *Free Radic. Biol. Med.* 47 (2009) 103–113, <https://doi.org/10.1016/j.freeradbiomed.2009.04.014>.
- R. Zhuang, L. Guo, J. Du, S. Wang, J. Li, Y. Liu, Exogenous hydrogen sulfide inhibits oral mucosal wound-induced macrophage activation via the NF- $\kappa$ B pathway, *Oral Dis.* 24 (2018) 793–801, <https://doi.org/10.1111/odi.12838>.
- R.M. Johnstone, The Jeanne Manery-Fisher Memorial Lecture 1991. Maturation of reticulocytes: formation of exosomes as a mechanism for shedding membrane proteins, *Biochem. Cell. Biol.* 70 (1992) 179–190, <https://doi.org/10.1139/o92-028>.

- [29] Y. Zhang, H. Liu, X. Liu, Y. Guo, Y. Wang, Y. Dai, J. Zhuo, B. Wu, H. Wang, X. Zhang, Identification of an exosomal long non-coding RNAs panel for predicting recurrence risk in patients with colorectal cancer, *Aging (Albany NY)* 12 (2020) 6067–6088, <https://doi.org/10.18632/aging.103006>.
- [30] Y. Xiong, L. Chen, C. Yan, W. Zhou, T. Yu, Y. Sun, F. Cao, H. Xue, Y. Hu, D. Chen, B. Mi, G. Liu, M2 Macrophagy-derived exosomal miRNA-5106 induces bone mesenchymal stem cells towards osteoblastic fate by targeting salt-inducible kinase 2 and 3, *J. Nanobiotechnol.* 18 (2020) 66, <https://doi.org/10.1186/s12951-020-00622-5>.
- [31] R. Yang, C. Qu, Y. Zhou, J.E. Konkel, S. Shi, Y. Liu, C. Chen, S. Liu, D. Liu, Y. Chen, E. Zandi, W. Chen, Y. Zhou, S. Shi, Hydrogen sulfide promotes Tet1- and tet2-mediated Foxp3 demethylation to drive regulatory T cell differentiation and maintain immune homeostasis, *Immunity* 43 (2015) 251–263, <https://doi.org/10.1016/j.immuni.2015.07.017>.
- [32] R. Yang, Y. Liu, T. Yu, D. Liu, S. Shi, Y. Zhou, Y. Zhou, Hydrogen sulfide maintains dental pulp stem cell function via TRPV1-mediated calcium influx, *Cell Death Dis.* 4 (2018) 1, <https://doi.org/10.1038/s41420-018-0071-4>.
- [33] B.D. Paul, S.H. Snyder, H<sub>2</sub>S signalling through protein sulphydration and beyond, *Nat. Rev. Mol. Cell Biol.* 13 (8) (2012 Jul 11) 499–507, <https://doi.org/10.1038/nrm3391>.
- [34] D. Zhang, J. Du, C. Tang, Y. Huang, H. Jin, H<sub>2</sub>S-Induced sulphydration: biological function and detection methodology, *Front. Pharmacol.* 8 (2017 Sep 6) 608, <https://doi.org/10.3389/fphar.2017.00608>.
- [35] B.D. Paul, S.H. Snyder, Protein sulphydration, *Methods Enzymol.* 555 (2015) 79–90, <https://doi.org/10.1016/bs.mie.2014.11.021>. Epub 2015 Jan 14.
- [36] M. Yu, H. Du, B. Wang, J. Chen, F. Lu, S. Peng, Y. Sun, N. Liu, X. Sun, D. Shiyun, Y. Zhao, Y. Wang, D. Zhao, F. Lu, W. Zhang, Exogenous H<sub>2</sub>S induces hrd1 S-sulphydration and prevents CD36 translocation via VAMP3 ubiquitylation in diabetic hearts, *Aging Dis* 11 (2) (2020 Mar 9) 286–300, <https://doi.org/10.14336/AD.2019.0530>.
- [37] S. Louvet-Vallée, ERM proteins: from cellular architecture to cell signaling, *Biol. Cell.* 92 (2000) 305–316, [https://doi.org/10.1016/s0248-4900\(00\)01078-9](https://doi.org/10.1016/s0248-4900(00)01078-9).
- [38] X. Sun, K. Li, M. Hase, R. Zha, Y. Feng, B.Y. Li, H. Yokota, Erratum: suppression of breast cancer-associated bone loss with osteoblast proteomes via Hsp90ab1/moesin-mediated inhibition of TGFβ/FN1/CD44 signaling: erratum, *Theranostics* 13 (1) (2023 Jan 1) 16–19, <https://doi.org/10.7150/thno.79085>.
- [39] A. Gonda, J. Kabagwira, G.N. Senthil, N.R. Wall, Internalization of exosomes through receptor-mediated endocytosis, *Mol. Cancer Res.* 17 (2019) 337–347, <https://doi.org/10.1158/1541-7786.MCR-18-0891>.
- [40] C. Barrès, L. Blanc, P. Bette-Bobillo, S. André, R. Mamoun, H.-J. Gabius, M. Vidal, Galectin-5 is bound onto the surface of rat reticulocyte exosomes and modulates vesicle uptake by macrophages, *Blood* 115 (2010) 696–705, <https://doi.org/10.1182/blood-2009-07-231449>.
- [41] D. Zech, S. Rana, M.W. Büchler, M. Zöller, Tumor-exosomes and leukocyte activation: an ambivalent crosstalk, *Cell Commun. Signal.* 10 (2012) 37, <https://doi.org/10.1186/1478-811X-10-37>, 10.1158/0008-5472.CAN-12-1040.
- [42] W.M. Henne, N.J. Buchkovich, S.D. Emr, The ESCRT pathway, *Dev. Cell* 21 (1) (2011 Jul 19) 77–91, <https://doi.org/10.1016/j.devcel.2011.05.015>.
- [43] J. Schöneberg, I.H. Lee, J.H. Iwasa, J.H. Hurley, Reverse-topology membrane scission by the ESCRT proteins, *Nat. Rev. Mol. Cell Biol.* 18 (1) (2017) 5–17, <https://doi.org/10.1038/nrm.2016.121>. Epub.2016.Oct5.
- [44] X. Zhu, F.C. Morales, N.K. Agarwal, T. Dogruluk, M. Gagea, M.-M. Georgescu, Moesin is a glioma progression marker that induces proliferation and Wnt/β-catenin pathway activation via interaction with CD44, *Cancer Res.* 73 (2013) 1142–1155.
- [45] Z. Luo, X. Shang, H. Zhang, G. Wang, P.A. Massey, S.R. Barton, C.G. Kevil, Y. Dong, Notch signaling in osteogenesis, osteoclastogenesis, and angiogenesis, *Am. J. Pathol.* 189 (2019) 1495–1500, <https://doi.org/10.1016/j.ajpath.2019.05.005>.
- [46] G. Chen, C. Deng, Y.-P. Li, TGF-β and BMP signaling in osteoblast differentiation and bone formation, *Int. J. Biol. Sci.* 8 (2012) 272–288, <https://doi.org/10.7150/ijbs.2929>.
- [47] R. Yang, T. Yu, X. Kou, X. Gao, C. Chen, D. Liu, Y. Zhou, S. Shi, Tet1 and Tet2 maintain mesenchymal stem cell homeostasis via demethylation of the P2rx7 promoter, *Nat. Commun.* 9 (1) (2018 Jun 1) 2143, <https://doi.org/10.1038/s41467-018-04464-6>.